Utilization of Geographic Information Systems and Manning Approach for Pico Hydro Energy Potential Mapping

Dewi P. Sari, Stevanus N. Jati, Imam Syofii, and Dendy Adanta, *Member IAENG*

***Abstract*—Applying pico hydro as a power plant in rural or remote areas to generate electricity is a possible solution. However, pico hydro is rarely applied because it is alleged that the funds needed are large for the energy potential survey due to requiring many human resources and the high risk of directly mapping meeting wild animals. Hence, a method is needed that can map the water-energy potential on a pico scale; this can accelerate the process of electrification in remote or rural areas. Thus, this study proposed tool to determine water energy potential for head utility Geographical Information System (GIS) based on Digital Elevation Model National (DEMNAS) of the Republic of Indonesia data, and discharge utility Manning approach and rainfall data. The GIS can be used as decision support because a potential location is detected accurately and precisely, and Manning's approach can be used as early data available discharge. From the mapping results, two locations are applicable for pico hydro: the undershot waterwheel and the breastshot waterwheel. The two turbines implemented presented good performance where the efficiency was close to their optimum limits.**

***Index Terms*—GIS, Pico Hydro, Potential Energy Mapping, DEM, Manning's approach**

I. Introduction

In 2019, there are 4.5 million Indonesians who do not yet have access to electricity [1]. This condition will be even more alarming if ignored since most live in rural or remote areas. In contrast, economic growth and improvement in living standards depend on electricity utilization [2]. To achieve energy sovereignty, the Ministry of Energy and Mineral Resources of Indonesia's strategic plan states the importance of new and renewable energy in achieving a 100% electrification ratio. From the survey, remote areas in Indonesia provide a lot of potential energy sourced by water [1], [3]. Most remote villages in Indonesia are located near rivers [4]. The river is used as a source of water used for daily purposes such as bathing, cooking, farming, hunting fish, etc. Hence Indonesian government used pico hydro turbines as an independent power plant because villages provide potential water energy.

Pico hydro is hydroelectricity with an output under 5 kW (< 5 kW). Countries with remote areas use pico hydro for electrification because it's a good solution [5], [6]. Compared to building a large power plant and transmitting it to remote areas, a mass installation of pico-hydro turbines may provide a more efficient and effective alternative [7].

Pico hydro is considered appropriate for remote areas in Indonesia based on a survey initiated by the State Electricity Company (Persero) of Indonesia (PT. PLN). PT. PLN increased the electrification ratio of West Papua Province where initially in 2017 it was 60.74 %, and in 2019 it would be 94 % [8]. The survey was conducted by 165 students, 100 soldiers (TNI), and 130 volunteers [9]. This survey to map the potential of local energy available in 1216 villages of West Papua Province. Two hundred ninety-two villages were surveyed In one week [9], the length of time needed because of the difficulty of the terrain to the villages. From the report, one village takes two days and two nights to reach it and must be reached via river [10]. Besides, the risk of meeting wild animals is also challenged in conducting surveys.

Pico hydro offers many advantages to contribute alternative electric energy as an off-grid source suitable for the poorly accessible area; this stimulates optimization the utilization of pico hydro continues. Efforts to optimize utilization of pico hydro such as proposed a method of reducing the operational failure risk with considered [11]: a design approach with a low-cost scheme; low equipment used; and the location should be capable of manufacturing turbines. Besides, an assessment of the turbulence model for the computational fluid dynamics method of each turbine was conducted, this for the design and prediction was accurate and fast [5]. Based on the assessment, the turbulence model for each turbine is the difference to get an accurate prediction: overshot waterwheel is recommended using standard k-ε; cross-flow turbine and undershot waterwheel using Renormalization Group (RNG) k-ε; and propeller, Pelton, Turgo, breastshot waterwheel, and Archimedes turbine using shear stress transport (SST) k-ω. The feasibility of the pico hydro electrical system is an important concern; the review results proposed that a direct current (DC) electrical system using a storage system based

Manuscript received October 20, 2021; revised March 24, 2022. This work was supported by Universitas Sriwijaya, Indonesia.

Dewi Puspita Sari is a lecturer in the Study Program of Mechanical Engineering Education, Faculty of Education and Teacher Training, Universitas Sriwijaya, Indralaya 30662, South Sumatera, Indonesia (e-mail: dewipuspita@fkip.unsri.ac.id).

Stevanus Nalendra Jati is a lecturer in the Study Program of Geological Engineering, Faculty of Engineering, Universitas Sriwijaya, Indralaya 30662, South Sumatera, Indonesia (e-mail: s.nalendra@unsri.ac.id).

Imam Syofii is a lecturer in the Study Program of Mechanical Engineering Education, Faculty of Education and Teacher Training, Universitas Sriwijaya, Indralaya 30662, South Sumatera, Indonesia (e-mail: imamsyofii@unsri.ac.id).

Dendy Adanta is a lecturer in the Department of Mechanical Engineering, Faculty of Engineering, Universitas Sriwijaya, Indralaya 30662, South Sumatera, Indonesia (corresponding author to provide phone: +62-711-580-062; e-mail: dendyadanta@ymail.com).

on batteries is a good agreement [7]. The batteries are easily distributed (lightly) to the rural or remote, and they can be stabilizers so that the supply voltage becomes stable (not fluctuate) [7].

Pico hydro is rarely applied because it is alleged that the funds needed are large for the site survey because they require a lot of human resources [8], [9]. Furthermore, the risk of directly mapping meeting wild animals is high. The mapping of the local energy potential is important because this is the key to increasing the electrification ratio in remote areas. Consequently, it requires indicators and tools to determine that practical reveal these potentials spatially. Therefore, a method is needed that can map the potential of water energy on a pico scale; this can accelerate the process of electrification in remote areas.

A map of pico hydro potential contribution as an off-grid source function of the local topographical feature. The topographical map was used to assess and measure potential elevation water energy (head) as a regional resource of potential. The potential regional plot (in the map) for the available head utility of geographic information system (GIS) and available discharge utility Manning's approach and rainfall data can be used as decision support to determine suitable technology for sites. Manning's approach was proposed because the prediction suing watershed feature in the GIS was inaccurate. After all, the river or irrigation width was small for the pico scale (under 2 m). Thus, this study proposed tool to determine water energy potential for head utility Geographical Information System (GIS) based on Digital Elevation Model National (DEMNAS) of the Republic of Indonesia data, and discharge utility Manning approach and rainfall data.

II. Method

Determination of the energy potential of hydropower should identify the characteristics of the river. These characteristics include the discharge (Q) and head (H) or elevation differences. The river's availability of Q and H depends on the watershed area and the river slope. Consequently, the potential energy along the river will vary. Therefore, it is reasonable to attribute energy potential to a watershed and use it as the pico-hydro energy potential spatial unit.

A. Head Determination

Determination of H_p for each vertex is an elevation difference of vertex p to the pertaining upstream vertex:

$$H_p = z_{upstream} - z_{downstream} \quad (1)$$

where $z_{upstream}$ is the elevation upstream, and $z_{downstream}$ is the elevation downstream. The further go upstream, the higher obtain H and the power. So, the upstream point must be determined correctly. There are two alternatives in selecting the upstream point, first, by setting certain distance conditions upstream. Second, by setting certain conditions of height difference upstream. The first alternative does not guarantee a point that will produce enough to be used as the head of a turbine. Thus, the second alternative is more feasible. For practical reasons, the vertex points at the upstream of the nearest downstream point higher than the specified condition will be used as the upstream point.

Once the upstream point is selected and the downstream is determined, then the irrigation slope angle (α) is known. The straight distance of the upstream to downstream (x) or called the vertex.

B. Discharge Determination

Discharge (Q) information is required to the determined potential energy of a certain river. The river flow used for the pico hydro (<5 kW) is irrigation so that Manning's formulation predicts the discharge (Q). The irrigation is a 2-stage trapezoidal shape so that the average of the stream water velocity (V) in irrigation using Manning's formulation-standard international (see (2)).

$$V = \frac{1}{n} \cdot R^{0.66} \cdot S^{0.5} \cdot c \quad (2)$$

where n is the roughness coefficient, R is the hydraulic radius, S is the slope, and c is the correction factor of 0.04. The Slope (S) is a determined derivative of m against x (dm/dx). R is a function of irrigation geometry (see (3)).

$$R = \frac{A}{u} \quad (3)$$

where A is the stream area, and u is the wetted perimeter. Since the irrigation is in the 2-stage trapezoidal shape, A becomes (4):

$$A = \frac{\left[b_1 + b_2 \;\; y_1 \right] + \left[b_3 + b_4 \;\; y_2 + y_1 \right]}{2} \quad (4)$$

b_1, b_2, b_3, b_4, y_1, and y_2 can be seen in Figure 1.

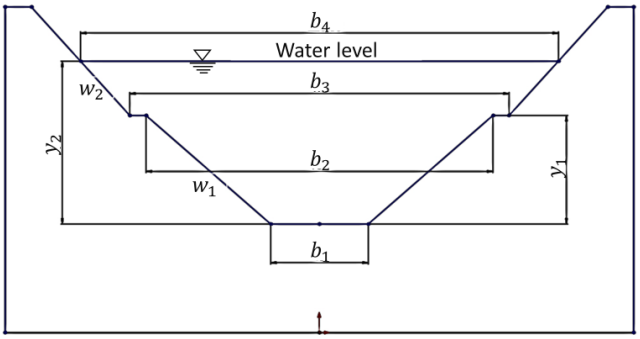

a. Schematic

b. Irrigation condition

Fig. 1. Batu Roto village irrigation

u (wetted perimeter) is the length of the irrigation surface submerged by water; the bigger u, the greater the friction losses irrigation. Based on Figure 1, the calculation u using (5):

$$u=b_1+2w_1+2\ b_3-b_2\ +2w_2 \quad (5)$$

where $w_1^2 = (b_2 - b_1)^2 + y_1^2$, and $w_2^2 = (b_4 - b_3)^2 + (y_2 - y_1)^2$.

Thus, the prediction of Q becomes:

$$Q_{Manning}=V \cdot A \quad (6)$$

The average stream water velocity (V) prediction using the manning approach is verified by measuring current meters. A rational model is the estimated discharge (Q) from a certain watershed that can be explored paired with rainfall records. The method is simple and easy to understand and has been an Indonesian national standard (SNI) [12]. SNI stipulates the use of this model to predict watershed discharge up to 5,000 hectares [12].

Validation of discharge estimates using measurement results. The rectangular weir is used to measure discharge because of the trapezoidal shape of irrigation. Using the current meter or the buoy method will result in less precise data [13]. Details explaining the discharge measurement method can be seen in [14]–[16].

C. The Procedure of Potential Power

The energy potential of the pico hydro turbine (P_P) that can be generated at each vertex p is determined by:

$$P_P=\gamma \cdot Q \cdot H_p \quad (7)$$

where γ is the specific weight of water.

The discharge (Q) is assumed to be constant (assumption the irrigation condition is no outflow), while the H_P varies. Consequently, the P_P can vary per vertex. In this study, the H_P has been determined of 5 m, so that the x will vary from case to case to reveal a sufficient river network line. The H_P of 5 m to identify the water-energy potential to the smallest scale, the lower the value, the more creek will be disclosed. The disadvantage is that the complexity of the river flow will give more processing load.

The estimation of the head uses the ArcGIS hydrology model to predict the potential of water energy in Batu Roto Village irrigation. The elevation determination is obtained from DEMNAS (Digital Elevation Model National) of Indonesia. The ArcGIS process begins by determining the location's coordinates, case study Batu Roto village located in the 1984 WGS zone UTM Zone 48S. The first process is to make a watershed for the analysis of studies. The initial process starts from the filling function, where the fill ensures that basins and streams in a certain area are outlined correctly. This process is done by filling in the blanks of the cell or removing fake cells that do not match the surrounding surface trends. Next is the flow direction, which determines the flow direction from each raster cell, and flow accumulation, which delineates stream networks in elevation models. Flow accumulation works by calculating accumulated flow as the accumulated weight of all cells flowing into each downslope cell in the raster output. The algebra map process is then performed, where the algebra map is a spatial analyst tool to show the amount of river flow according to the desired density.

D. Performance Analysis

Four parameters are measured: current (a), voltage direct current (v_{dc}), wheel rotation (n), and torque (τ). These four parameters determine the mechanical power (P_{mech}) and the electrical power (P_{elec}). The a and v_{dc} were measured using the DM-133D multimeter with accuracy is categorized as a percentage of 0.5%. The n was measured using a tachometer DT-2334C+ with accuracy is categorized as a percentage of 0.05%. The τ was measured using a Prony brake system (see Figure 6-a), where the scale used is a high-precision strain gauge sensor system with a maximum capacity of 100 kg with an accuracy of 0.05 kg (reading), equipment configuration can be accessed in [14], [15]. The loading is carried out 31 times with a maximum load of 60 kg.

The P_{mech} is a function of ω and τ:

$$P_{mech}=\tau \cdot \omega \quad (8)$$

where ω is the angular velocity of the wheel ($\omega=2 \cdot \pi \cdot n/60$). Whereas the P_{elec} is a function of a and v_{dc}:

$$P_{elec}=a \cdot v_{dc} \quad (9)$$

Finally, turbine performance is the ratio between P_{mech} and P_{elec} with the net power $P_{nett,}$ for example:

$$\eta_{elec} = P_{elec} / P_{netto} \cdot 100\% \quad (10)$$

The P_{netto} is the amount of waterpower converted by the turbine; for the undershot waterwheel, the P_{netto} is $0.5 \cdot \rho \cdot A_{blade} \cdot V^3$ and for the breastshot waterwheel is $\gamma \cdot Q \cdot H_{netto}$.

III. Information Geographic of Batu Roto Village

The Batu Roto villages, Hulu Palik District, North Bengkulu-Indonesia, were used as a case study to determine the GIS's reliability. The Batu Roto villages are in 3°28'13.0"S 102°17'23.7"E, where its distance to district government centre is 4 km, distance to regency government centre is 17 km, and distance to province government centre is 65 km (see Figure 2). The Batu Roto village was chosen because it was an electricity crisis area [14], [15]. Although there is a national electricity grid, street lighting is insufficient. It is hoped that the study results can serve as suggestions for the Government of North Bengkulu and other similar regions (having the water-energy potential and experiencing an electricity crisis). The total length of Batu Roto village irrigation ± 5800 m for 180 Ha of rice fields [17].

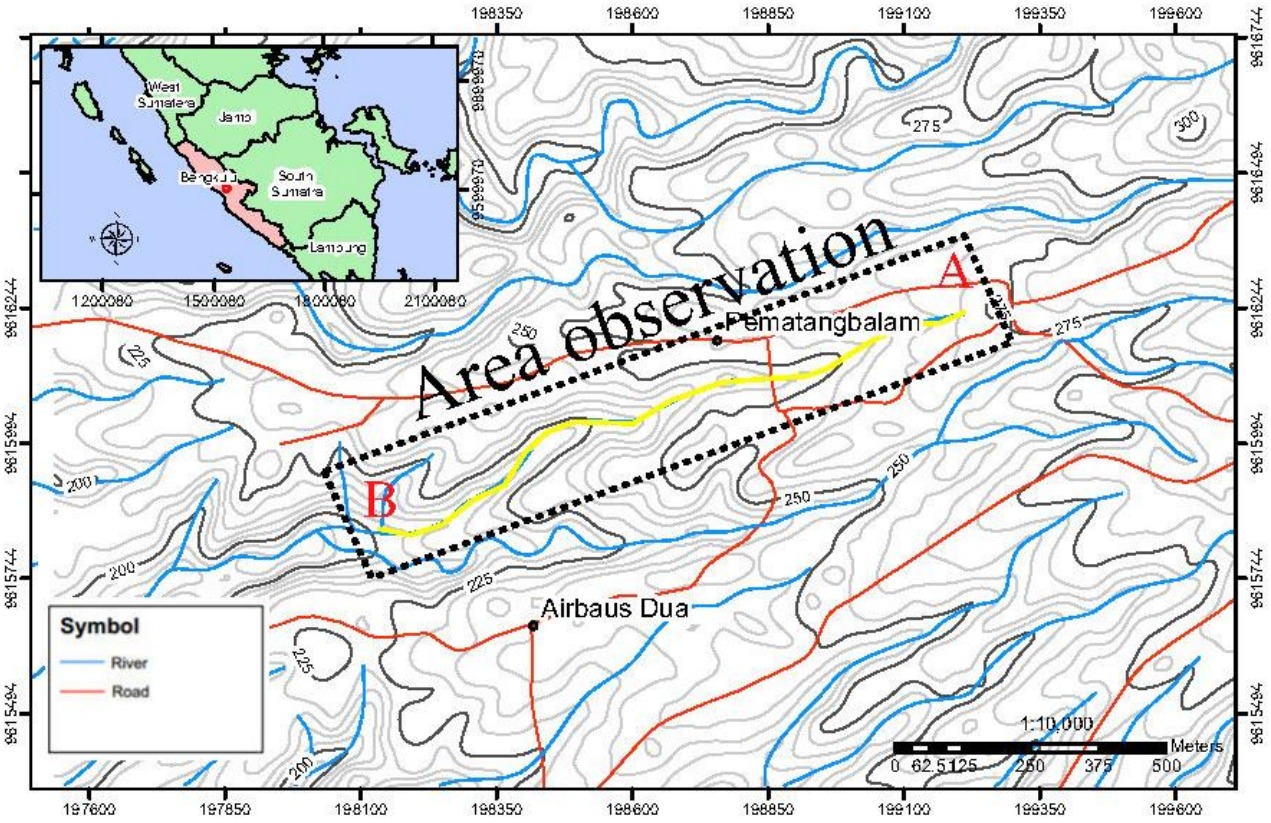

Fig. 2. Location of Batu Roto villages irrigation

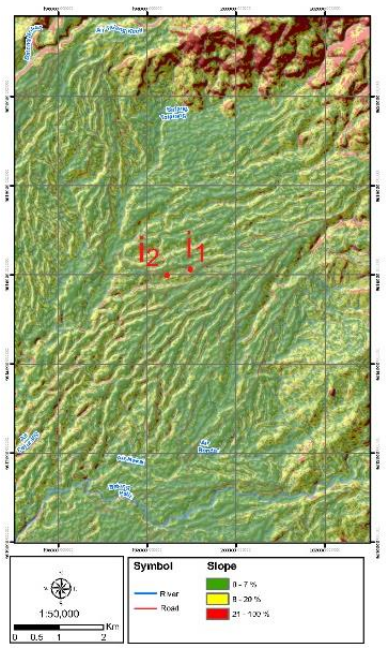

a. Computing result

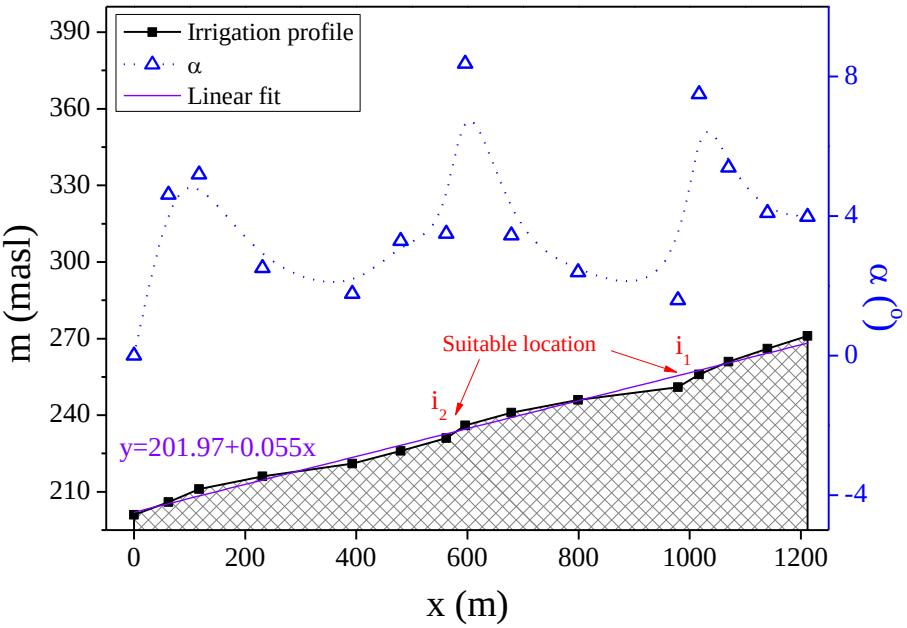

b. Elevation of irrigation

Fig. 3. Elevation and irrigation slope angle by DEMNAS

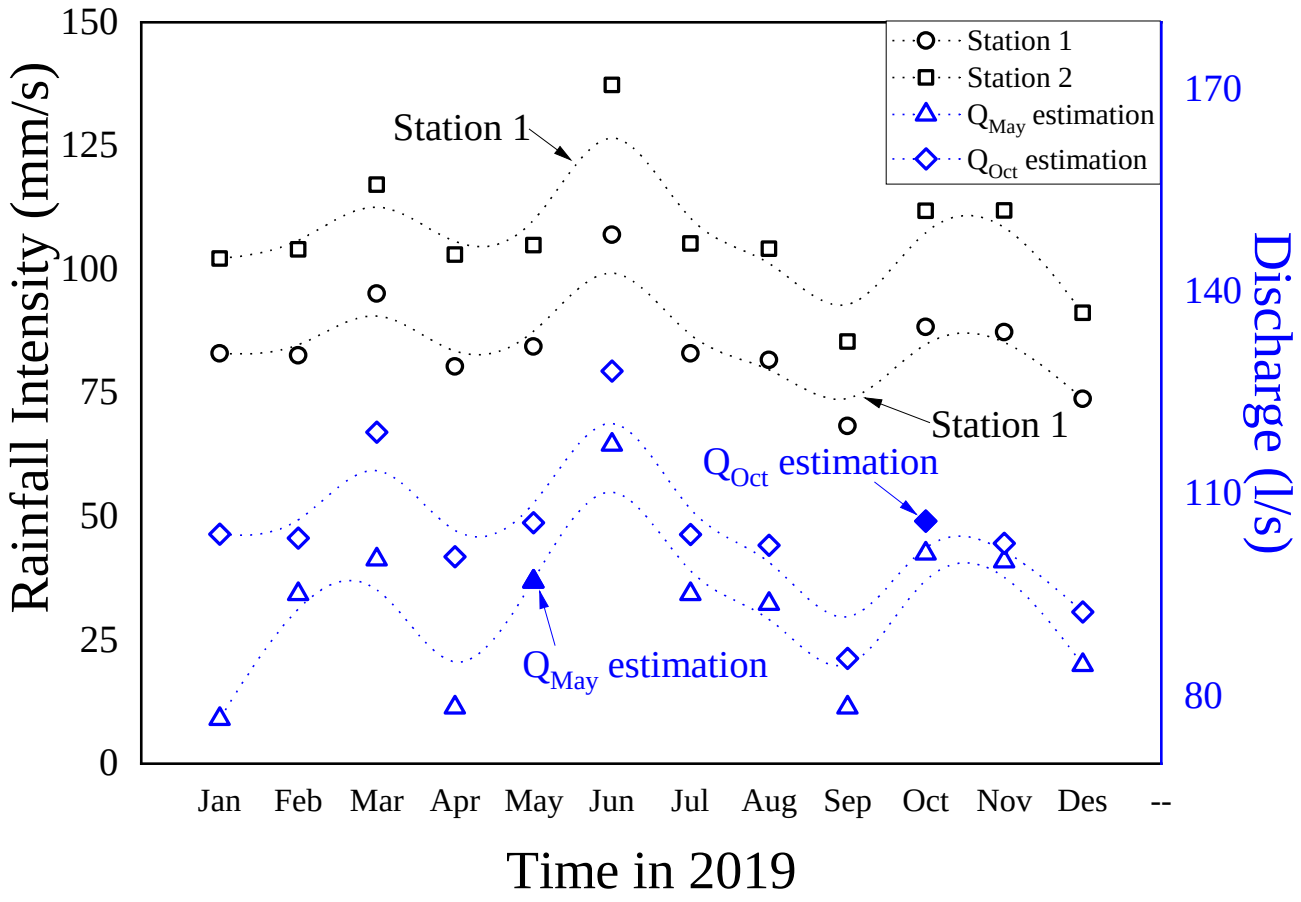

Fig. 4. Discharge available prediction using rainfall distribution

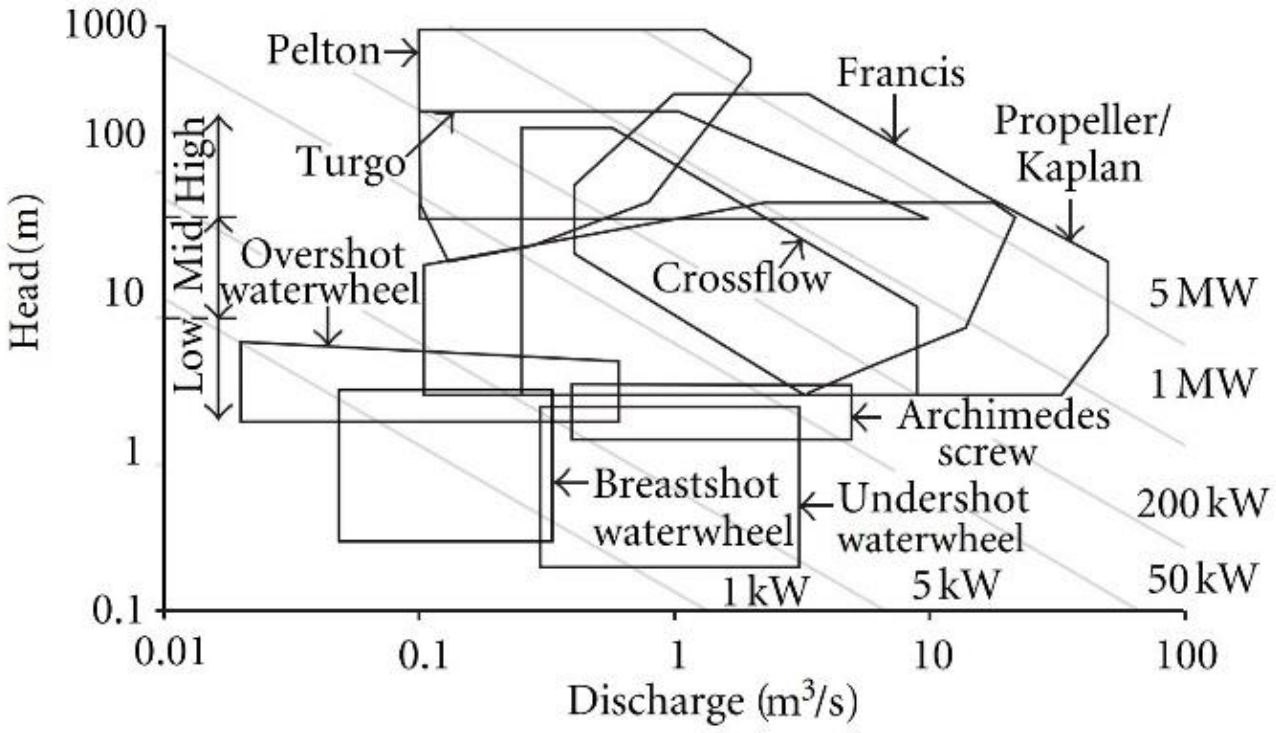

Fig. 5. Relation of discharge into the head [18]

Distance projection used spatial digitation to visualize distance with precision and accuracy [19], [20]. From Figure 2, the length of the irrigation is measured spatially. Next, the upstream and downstream elevation of the observed irrigation is determined. In this case, the elevation grid (digitization) used is 5 m (see Fig. 3-b). Each digitizing result is called a vertex. The vertices are then projected using contour digitization. Projection of elevation results from the configuration of satellite image data by Digital Elevation Model National (DEMNAS). The DEMNAS is the primary data source for watershed analysis because it can describe elevation of ground (land) in detail [21]. The DEMNAS data can be accessed at http://tides.big.go.id. Digitized data is visualized using remote sensing referring to one map policy, this data is downloaded at http://tanahair.indonesia.go.id/portal-web.

IV. Water Energy Potential in Batu Roto Irrigation

A. Head Potential

Based on the mapping results using DEMNAS, the distance (x) from point A to B of Figure 2 is 1212 m. Point A is at an altitude of 271 meters above sea level (masl) and point B of 201 masl. Based on numerical calculation of DEMNAS, the boundary conditions for the H_{min} are 5 m for point A to B resulting in 14 vertices, where the minimum irrigation slope angle (α) is 1.59°, and the maximum is 8.37° with an average of 3.84° (see Figure 3).

Based on morphology aspects, vertices 4 and 8 are suitable areas for pico hydro turbine installation (Figure 3). Since the α is high and x is relatively short [13], the water kinetic energy is relatively higher than other areas.

Based on Figure 3, the m has a relation to the x, expressed m=201.97+0.055x (first-order). Therefore, the dm/dx for Equation 2 is 0.055 (S=0.055); this indicates that the morphology of irrigation is gentle (not steep), which is presentable with the mapping results using DEMNAS (α average of 3.84°).

B. Discharge Estimation

From the field survey, it is known that the sizes b_1, b_2, b_3, b_4, y_1, and y_2 are 0.3 m, 0.6 m, 0.9 m, 1.2 m, 0.3 m, and 0.5 m, respectively. Figure 1 and the field survey show that w_1 and w_2 are 0.42 m and 0.36 m, respectively, determined using the Pythagoras theorem. Based on Equation 4 and Equation 5 using field survey data, the area of the stream through the trapezoidal irrigation (A) is 0.975 m^2, and its wetted perimeter (u) is 2.47 m. Therefore, the average water stream velocity ($V_{Manning}$) prediction using Equation 2 is 0.126 m/s, where the magnitude of the parameter is S of 0.055, R of 0.395 m, n of 0.04 $s/m^{0.33}$, and c of 0.04. The n of 0.04 $s/m^{0.33}$ because although the irrigation walls were concrete semen, the irrigation bed has been covered by mud and the walls by moss. Thus, using the Manning formula ($Q_{Manning}$), the available discharge estimate is 0.126 m^3/s (125.8 l/s).

The field survey was conducted twice in May [15] and October 2019 [14]. In May 2019, the measured discharge (Q_{May}) was 0.097 m^3/s with the area of the stream (A_{May}) of 0.975 m^2 and the average water stream velocity (V_{May}) of 0.099 m/s [15]. Whereas, in October 2019, the measured discharge (Q_{Oct}) was 0.106 m^3/s with the area of the stream (A_{Oct}) of 0.116 m^2 and the average water stream velocity (V_{Oct}) of 0.91 m/s [14].

TABLE I
Comparison of Discharge Predicted with its Measurement Result

Parameters	Prediction	Measurement	
		May 2019	October 2019
A	0.975 m^2	0.975 m^2	0.91 m^2
V	0.13 m/s	0.10 m/s	0.12 m/s
Q	0.126 m^3/s	0.097 m^3/s	0.106 m^3/s

The discharge prediction using the Manning formula against the field survey has differences. The deviation of the May 2019 measurement to Manning's prediction is 13.95%, and for October is 18.9%. For Indonesia, the rainfall with a percentage deviation from its mean is ± 25% [22]. Hence these deviations (prediction with measured results) were considered insignificant since the measured discharge cannot be directly exploited when paired with rainfall data; this to determine the minimum discharge available in the river or irrigation to avoid water shortage supply for the operating turbine. Thus, the discharge prediction using the Manning formula for irrigation is feasible for this case.

Two stations are used to ensure the distribution of the average monthly rainfall. The two stations' rainfall distribution showed a similar pattern (see Figure 4). From Figure 4, the exploitable discharge is 76.56 l/s.

C. Analysis of Exergy of Water and Pico Hydro Technology

Head for pico-hydro power is available along with the irrigation of Baturoto (see Figure 3), all the way from it is upstream up to downstream. The pico-hydro turbine cannot use the whole available Q and H provided by the irrigation. Moreover, the slope (S) of 0.055 expresses that the irrigation slope angle (α) is 3.15°, categorized as sloping (ramps). This condition proposes the effective head is 10% of the available head. Therefore, based on Figure 3 with H_{eff} 10% from H_{avai} and Q_{avai} of 76.56 l/s (0.07656 m^3/s), throughout the Batu Roto irrigation, 14 locations were identified as having a potential of 375.53 W.

There are two suitable locations for the turbine implemented; both locations have x lengths of 32 m (i_1) and 38 m (i_2), respectively. The i_1 and i_2 are considered because x is small. Consequences, losses due to friction between water and irrigation walls are lower than in other locations.

Based on Figure 5, the undershot waterwheel and breastshot waterwheel are suitable technologies for a H_{avai} of 0.5 m and Q_{avai} of 0.07656 m^3/s. The undershot waterwheel is a water turbine that absorbs water kinetic energy (hit) and hydrodynamics force using the blade at the bottom [23], [24]. Whereas the breastshot waterwheel is a water turbine that absorbs weight (contain) and kinetic energy of water using the bucket at the centre [25], [26].

a. Undershot waterwheel

b. Breastshot waterwheel

Fig. 6. Implementation pico hydro in Batu Roto village irrigation

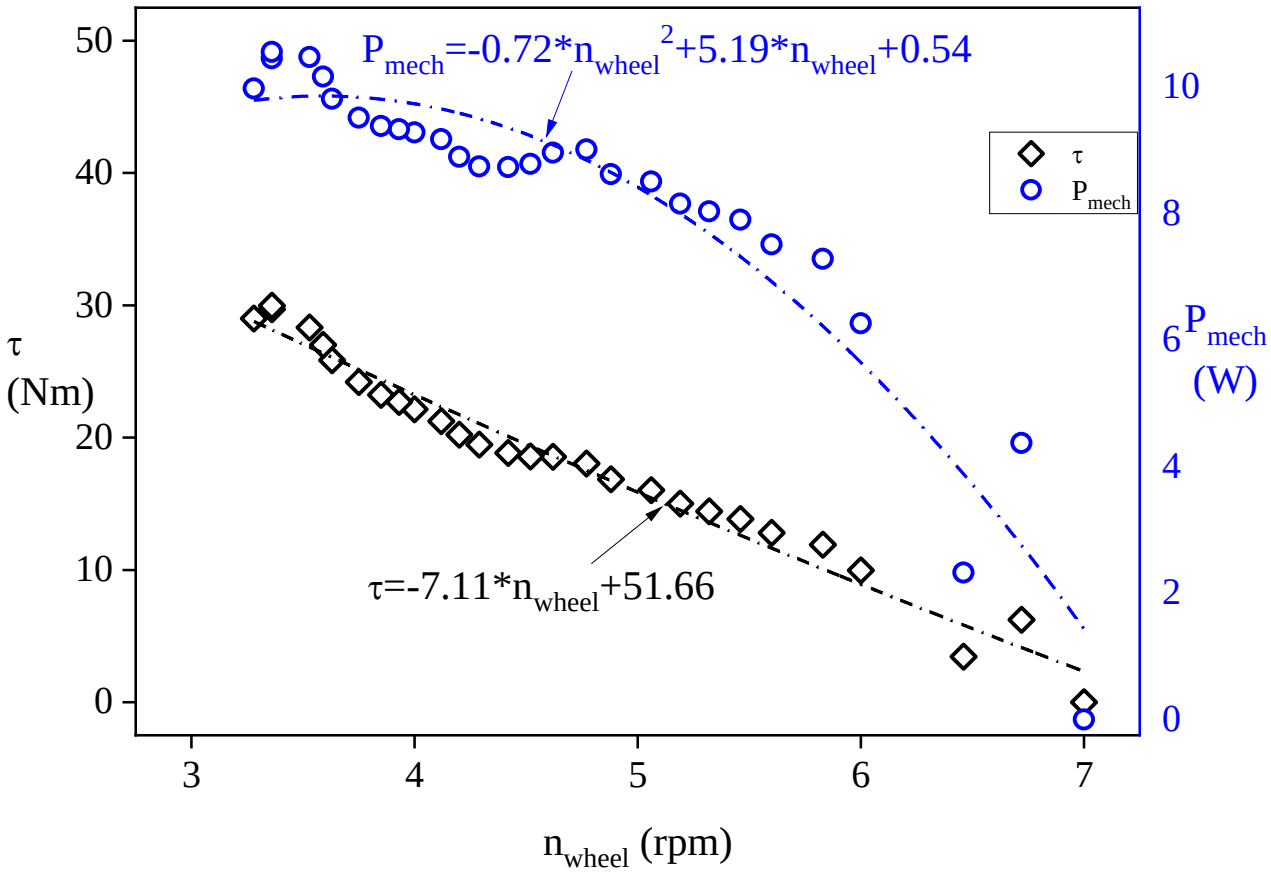

a. Mechanical power

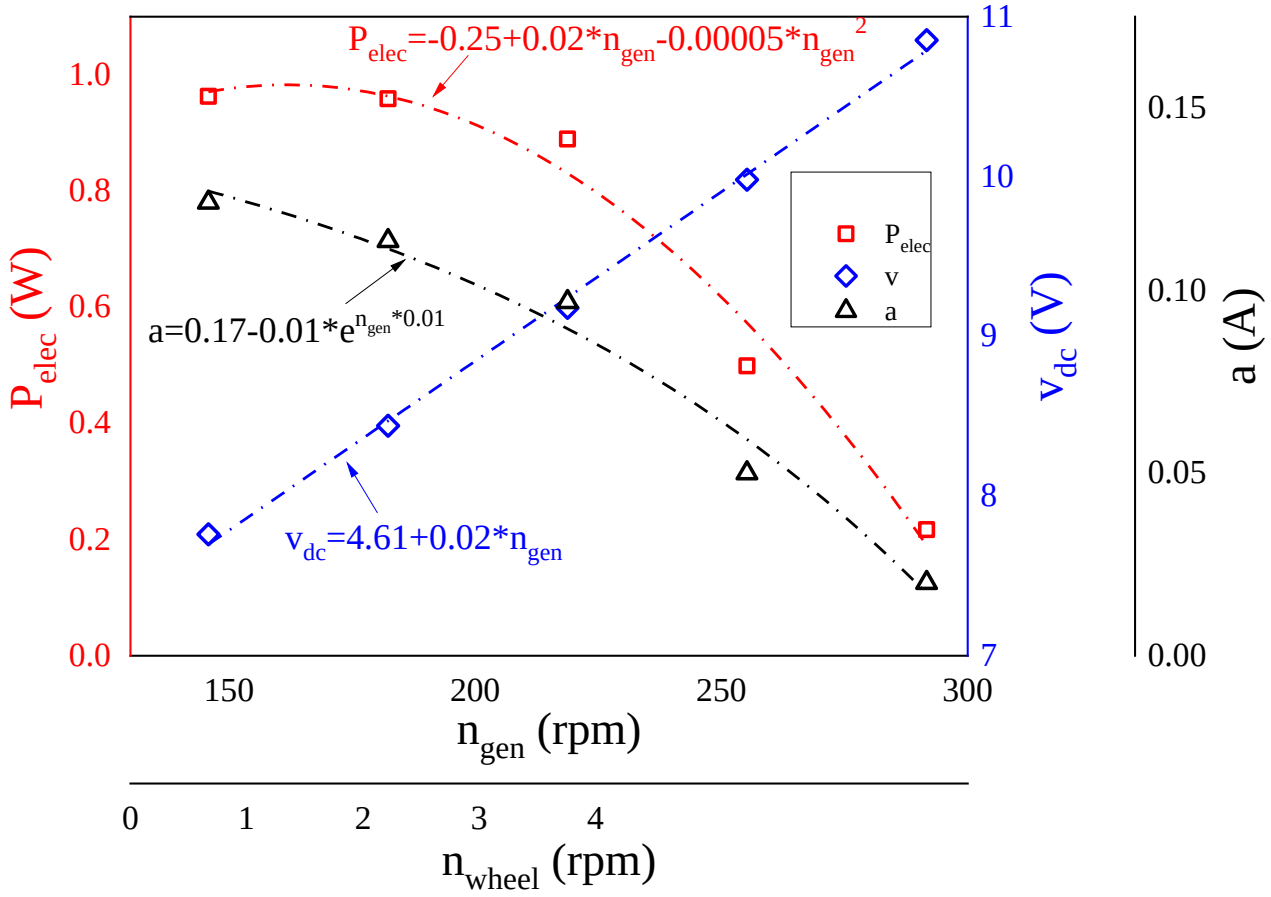

b. Electrical power

Fig. 7. The undershot waterwheel power

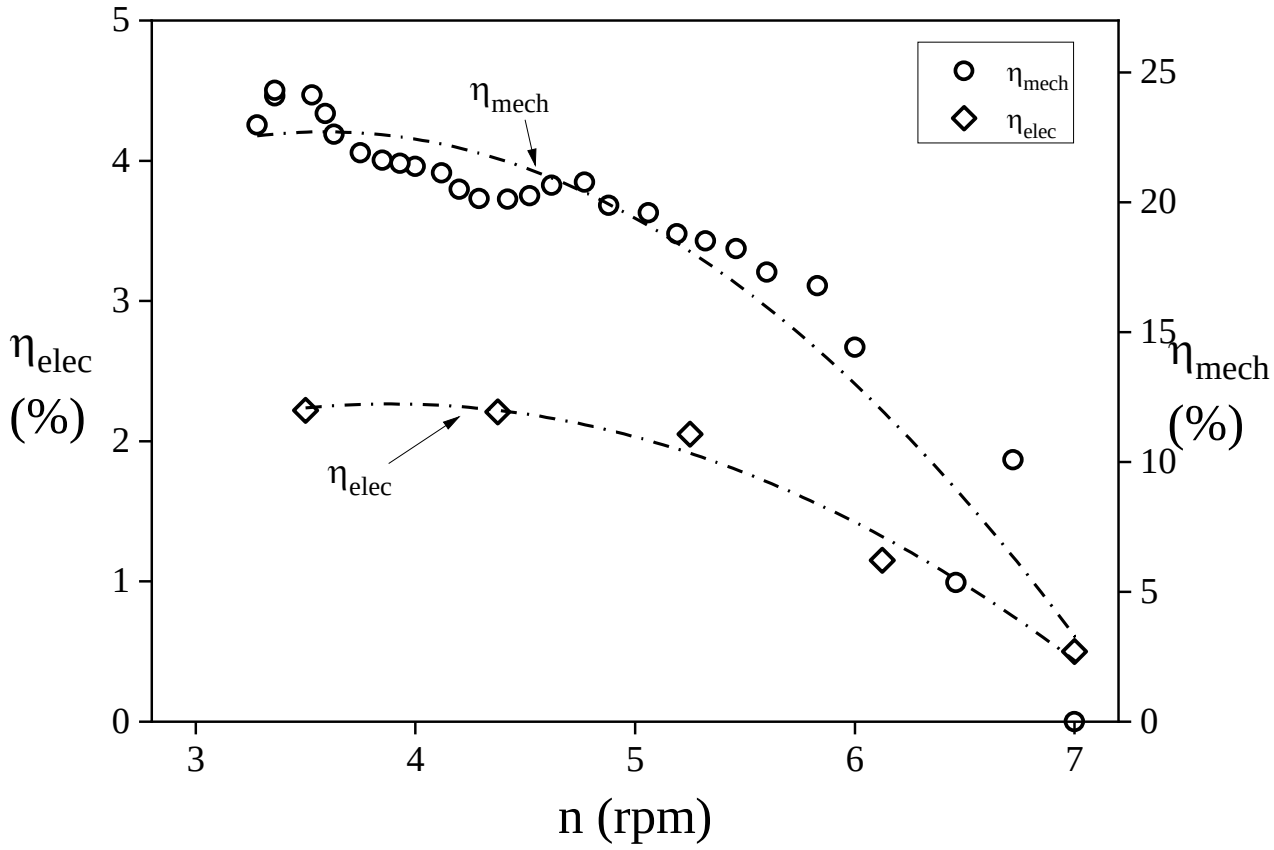

a. Mechanical and electrical efficiency

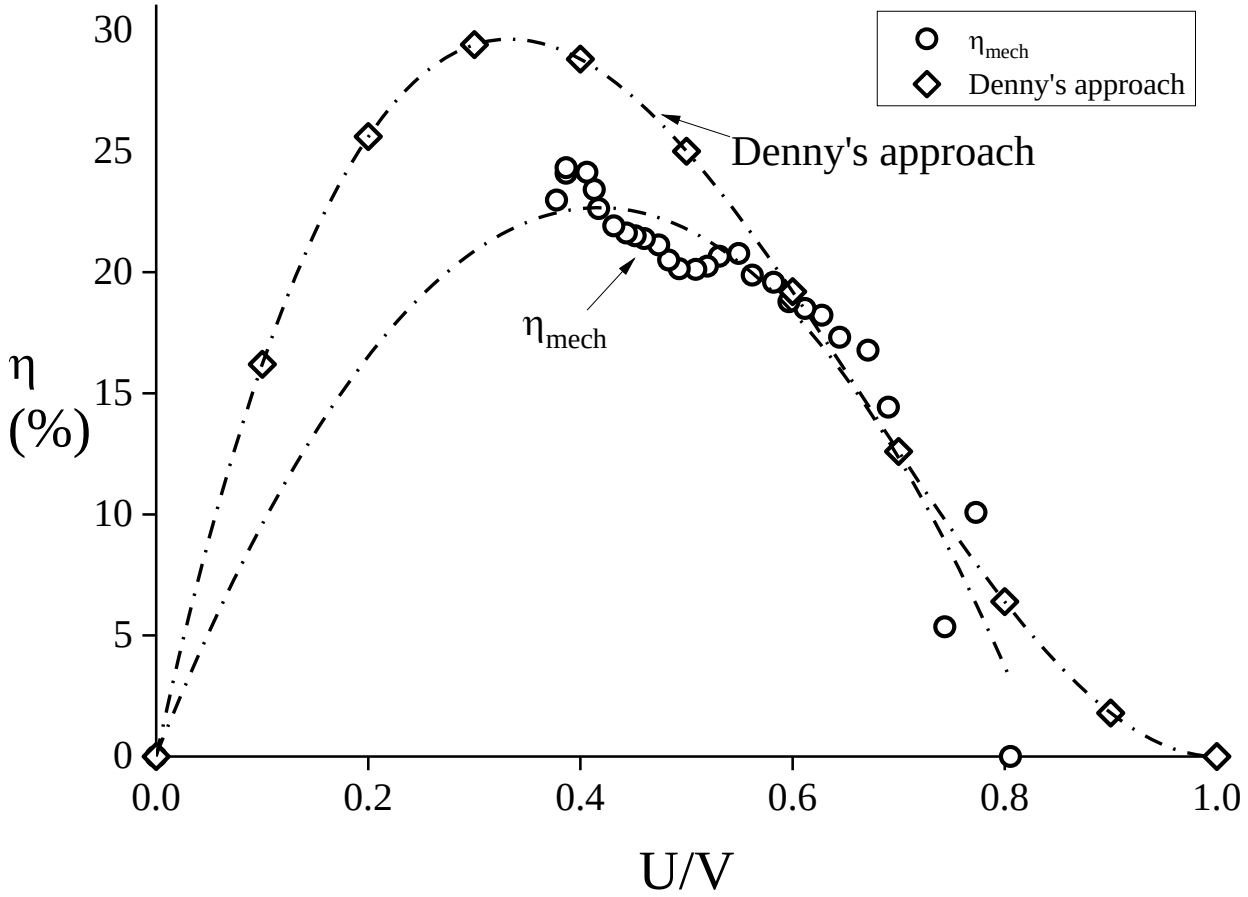

b. Verification to Denny's approach

Fig. 8. The undershot waterwheel performance

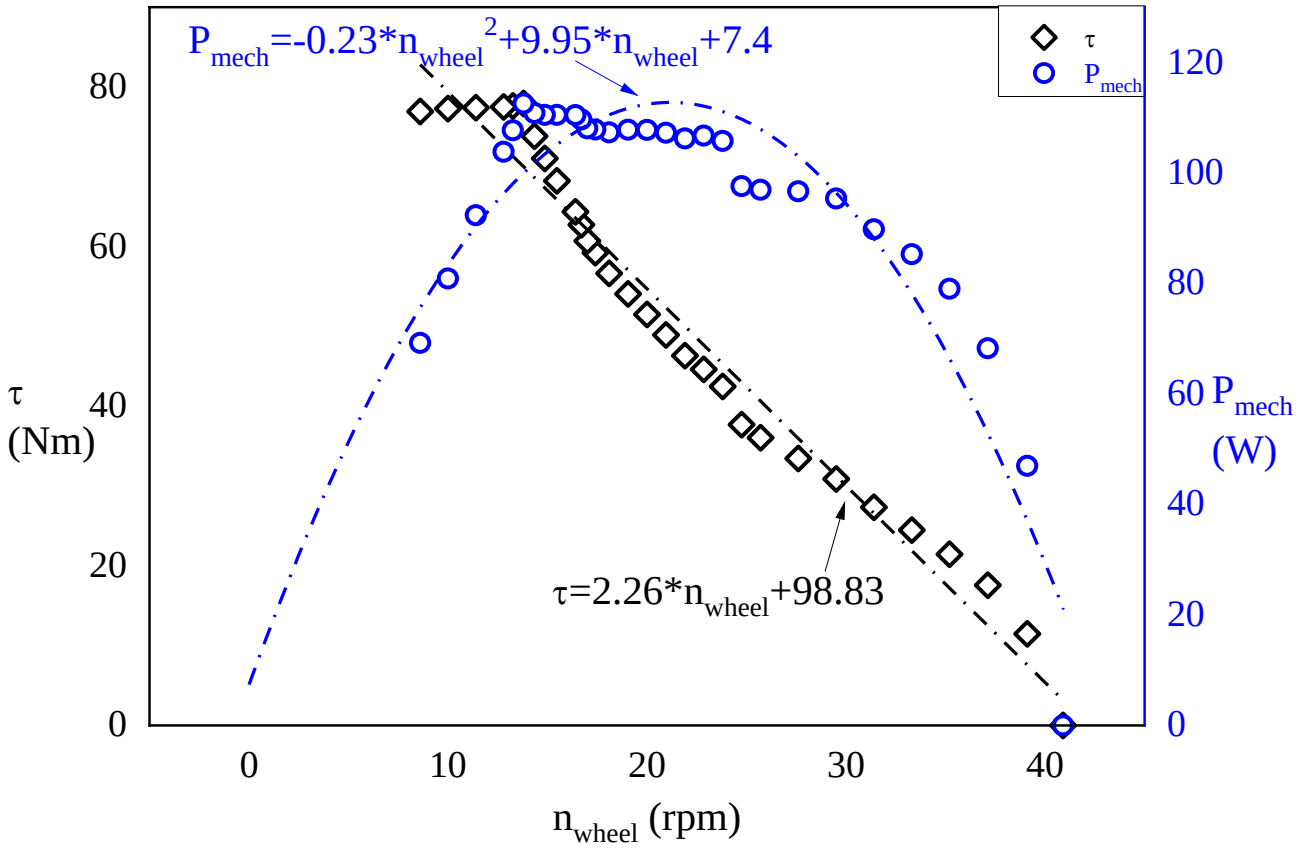

a. Mechanical power

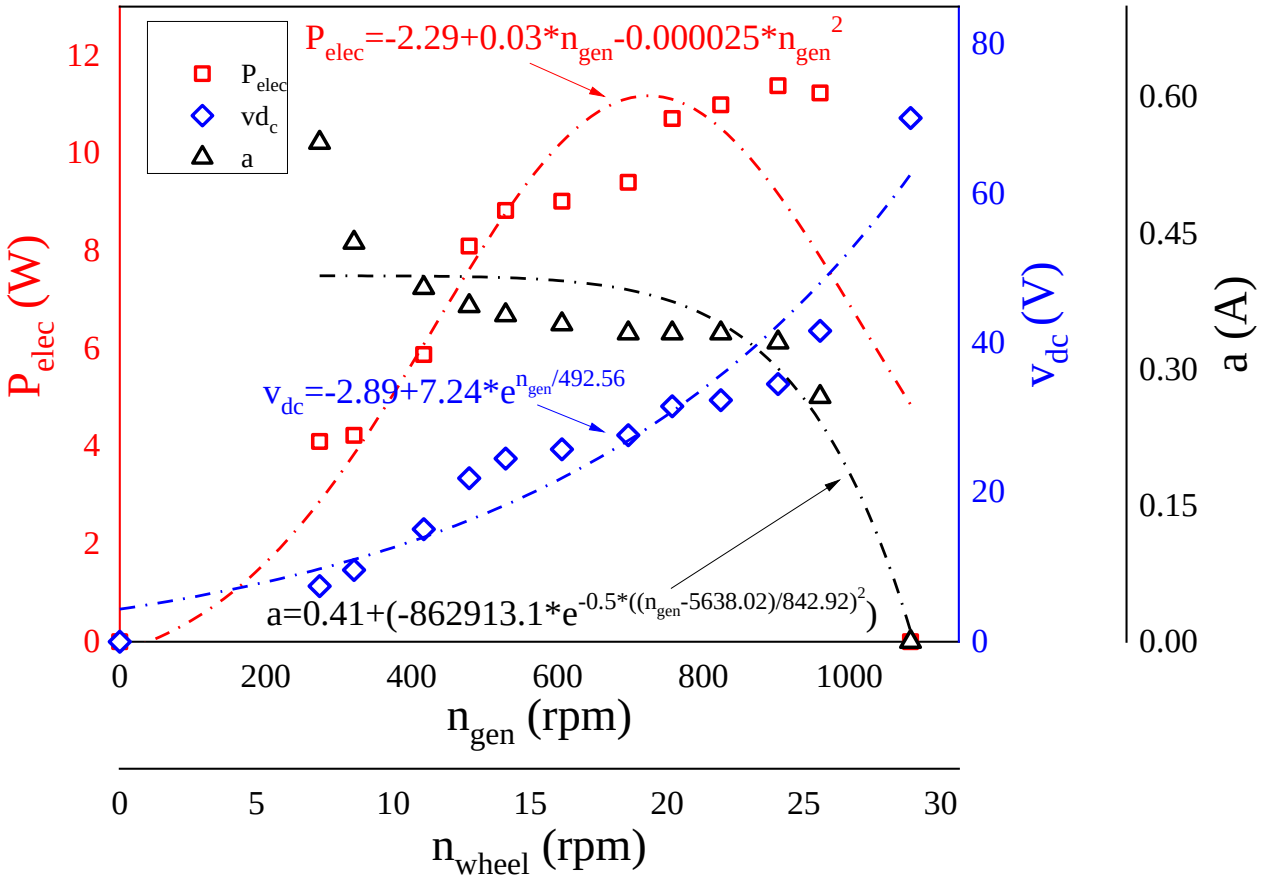

b. Electrical power

Fig. 9. The breastshot waterwheel power

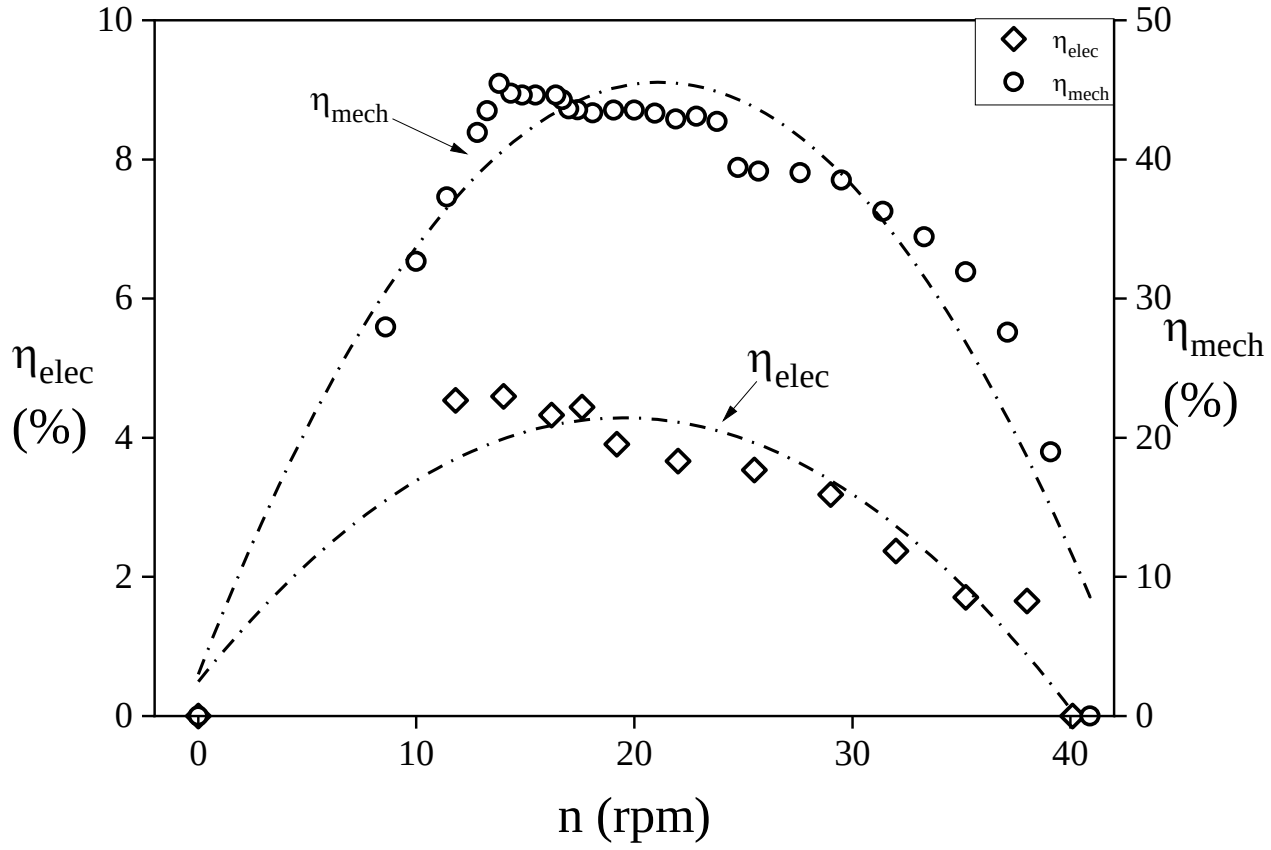

a. Mechanical and electrical efficiency

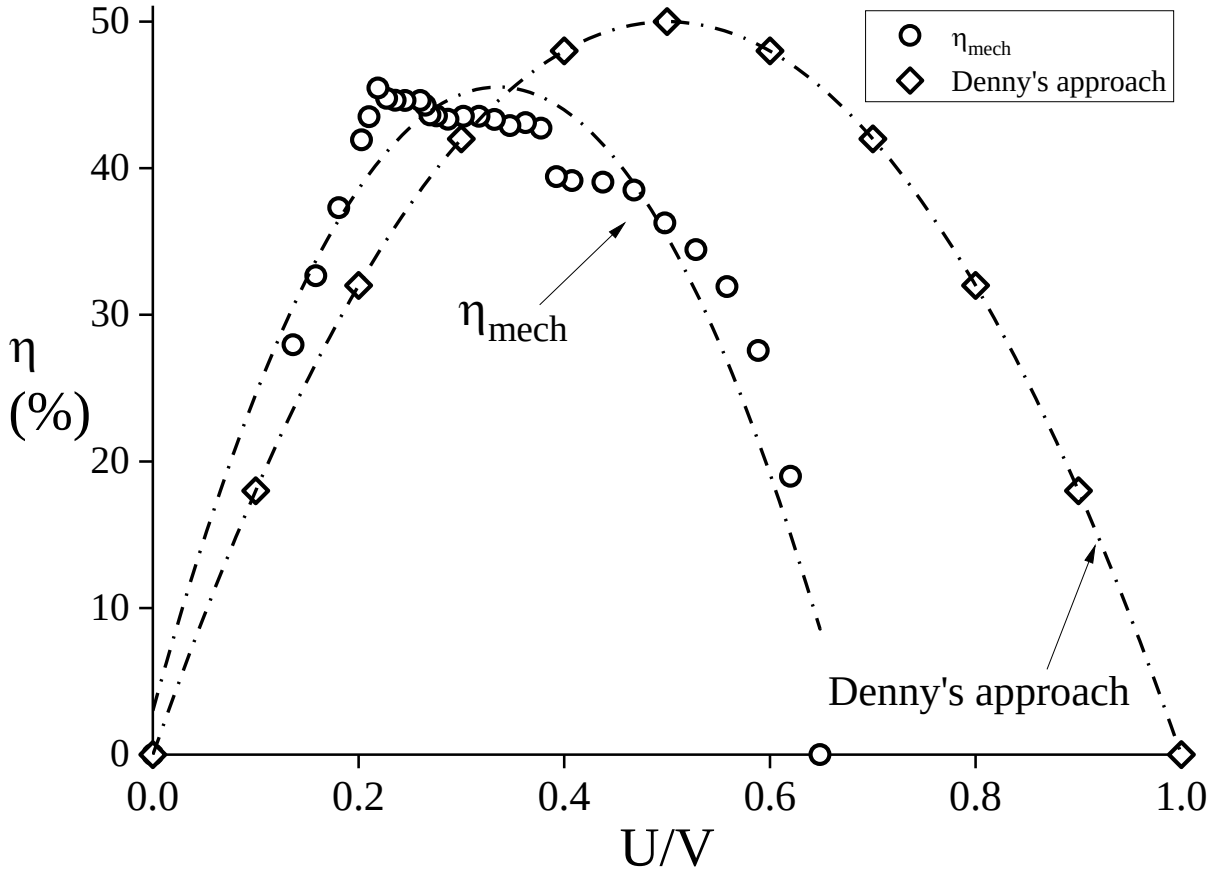

b. Verification to Denny's approach

Fig. 10. The breastshot waterwheel performance

The undershot waterwheel has a maximum efficiency of 55% lower than a breastshot waterwheel of 80% [27]. However, the undershot waterwheel is simpler, so it is easier to build than a breastshot waterwheel, which breastshot waterwheel has a complex geometry. Both technologies are applied as independent power plants in remote or rural areas because they are environmentally friendly [27]. Both have a low rotation with high torque, which is safe for aquatic biota [5].

V. Implementation Pico Hydro in Batu Roto

Based on Figure 3 that two vertices are suitable for pico hydro. The vertex i_1 for undershot waterwheel and vertex i_2 for breastshot waterwheel (see Figure 6). The undershot and breasthot waterwheel result in wheel-low rotation (large torque). Hence both turbines use a transmission system to meet the rotation DC generator requirements (minimum 150 rpm). Therefore, two levels of the transmission system are used (see Figure 6-b): pulley to a pulley (1:3) and pulley to a gearbox (1:12.5).

The undershot waterwheel used has a diameter (D) of 2 m, width (L) of 0.4 m, and 12 blades [14] (see Figure 6-a). Whereas the breastshot waterwheel used has a diameter (D) of 1.2 m, width (L) of 0.4 m, and 16 buckets [15]. Both turbines are made from iron steel available on the market, assembled using welding, and coated with corrosion-resistant paint. The investment cost for manufacturing the undershot waterwheel is USD 420 [14] and for a breastshot waterwheel is USD 620. The breastshot waterwheel is more expensive due to the need for more material (large bucket number and dimension) and the bucket manufacture complexity (see Figure 6-b).

A. Undershot Waterwheel Performance

Based on Figure 7-a, the results are similar to previous studies [23], [28], [29]. The relation of the wheel rotation (n_{wheel}) to the torque (τ) is a graphical linear function, and the mechanical power (P_{mech}) is parabolic. Based on Figure 7-a, the τ maximum of 29.01 N·m is reached at a n_{wheel} of 3.28 rpm, and the τ minimum of 3.43 N·m at a n_{wheel} of 6.46 rpm. The n_{wheel} without load generated is 7 rpm. Based on Figure 7-a, the highest mechanical power (P_{mech}) of the undershot waterwheel of 10.55 W is achieved at 3.36 rpm n_{wheel} and 29.97 N·m.

Based on Figure 7-b, voltage (v), current (a), and electrical power (P_{elec}) are affected by rotation (n_{wheel} and generator rotation (n_{gen})); this is similar to the previous studies [31][32], where the DC generator used is similar. The relation n_{gen} to v is a graphical linear function, the relation to a is exponential, and the relation to the P_{elec} is parabolic. Based on Figure 7-b, the highest P_{elec} was 0.96 W reached at 145.8 rpm n_{gen} (3.5 rpm n_{wheel}) with five loads (15 W lamp), the condition of all lamps was dim.

Based on Figure 8, the mechanical efficiency (η_{mech}) and electrical efficiency (η_{elec}) of the undershot waterwheel toward the n_{wheel} are parabolic. The highest η_{mech} was 24.3% reached at 3.36 rpm n_{wheel} and 29.01 N·m τ (load 60 kg), while the lowest η_{mech} was 2.32% reached at 6.46 rpm n_{wheel} and 3.43 N·m τ (load 2 kg). For the electrical efficiency (η_{elec}), the highest is 2.22 % (5 lamps) at 3.5 rpm n_{wheel}, 7.76 V_{dc} v, and 0.12 A a, while the lowest is 0.5% (1 lamp) at 7 rpm n_{wheel}, 10.8 V_{dc} v, and 0.02 A a. The more the load (lamp), the lamp is getting dimmer. Since the voltage received by each lamp is lower than required.

Figure 8-b is the verification results the Figure 8-a to Denny's approach [28], the limitation efficiency of the undershot waterwheel is $2 \cdot U/V(1-U/V)^2$, the U is wheel velocity. The verified data is mechanical efficiency. Based on Figure 8-b, the deviation of Denny's approach to undershot waterwheel performance is 5.09%, while the deviation in operating condition (U/V) is 0.09. The deviation is categorised as low, indicating that the method and test results for the undershot waterwheel are verified. Furthermore, Denny's approach's low deviation performance and operating condition show the turbine is working according to expectations. However, the study of the relation between the blade number and the moment of inertia of the wheel still necessary attention so that the undershot waterwheel performance is close to Denny's limit. Besides, the results obtained in Figure 8 are similar to previous studies [30] in which the optimum performance of the undershot waterwheel (Sagebien wheel) occurs at the U/V of 0.35 – 0.4. Thus, the recommended U/V for designing an undershot wheel is 0.35 – 0.4.

B. Breastshot Waterwheel Performance

Figure 9-a is similar to Figure 7-a, where the relation of the n_{wheel} to τ is a graphical linear function, and the n_{wheel} to the P_{mech} is parabolic. Based on Figure 9-a, the τ maximum of 77.94 N·m is reached at a n_{wheel} of 13.8 rpm, and the τ minimum of 11.483 N·m at a n_{wheel} of 39.1 rpm. The n_{wheel} without load, generated is 40.9 rpm. Based on Figure 7-a, the highest P_{mech} of the breastshot waterwheel of 112.58 W is achieved at 13.8 rpm n_{wheel} and 77.94 N·m.

Figure 9-b is the relation of v, a, and P_{elec} to n_{wheel} and n_{gen}. The relation n_{gen} to v is a graphical exponential function, the relation to a is Gauss, and the relation to the P_{elec} is parabolic. Based on Figure 9-b, the highest P_{elec} was 11.37 W reached at 902.2 rpm n_{gen} (24.06 rpm n_{wheel}) with eleven loads (33 W lamp), the condition of all lamps was dim. The n_{gen} of 902.2 rpm produces v of 34.48 Vdc and 0.33 A.

Based on Figure 8, the η_{mech} and the η_{elec} of the breastshot waterwheel toward the n_{wheel} are parabolic (similar to the undershot waterwheel). The highest η_{mech} was 45.47% reached at 13.8 rpm n_{wheel} and 77.94 N·m τ (48 kg load), while the lowest η_{mech} was 18.98% reached at 39.1 rpm n_{wheel} and 11.48 N·m τ (load 2 kg). At the condition of 24.06 rpm n_{wheel}, 34.48 V_{dc} v, and 0.33 A a, the highest electrical efficiency (η_{elec}) of 4.59% (2 lamps). In contrast, the lowest is 1.65% (11 lamps) at 7.31 rpm n_{wheel}, 7.45 V_{dc} v, and 0.55 A a. The more the load (lamp), the lamp is getting dimmer because the voltage received by lamps is lower than the required (minimum 12 Vdc); this condition is similar to the undershot waterwheel.

The breasthot waterwheel performance is verified using Denny's limit [28]. The Denny's limit for a breastshot waterwheel is $2 \cdot U/V(1-U/V)$ [28]. The difference in the limits of the two turbines is because the breastshot waterwheel performance is affected by gravity, contrary the undershot waterwheel is not [28]. The V for breastshot waterwheel limit cannot be used directly because the

breastshot has a head (H=0.5 m), so the becomes $V=V+(2\cdot g\cdot H)^{0.5}$. Based on Figure 10-b, the deviation of Denny's approach to breastshot waterwheel performance is 4.53%, and the deviation in operating condition (U/V) is 0.28 (in the percentage of 56.23%). The significant deviation for operating conditions of breastshot waterwheel was suspected because Denny considered the V analysis is not affected by the H. Furthermore, the results in Figure 10-b are similar to Quaranta and Revelli's (2016) studies [31], where the maximum operating conditions occurs at U/V of ± 0.29. The U/V of 0.28 to 0.29 is realistic for a breastshot waterwheel because a larger torque is required than runner rotation (gravity's influence). Thus, the recommended U/V for designing a wheel of breastshot is 0.28.

VI. Discussion

Mapping water energy potential using GIS can save time and money because the ideal location is well identified (see Figure 6). From the results, the projection of irrigation and its elevation by GIS-based on DEMNAS data is accurate and precise. This result is similar to the Jati et al. study [32] where GIS is capable of the map the water-energy potential location. It is predicted that two locations have energy potential, namely i_1 and i_2. The disadvantage of GIS cannot predict the discharge in pico and micro [32] scale because of the small irrigation width. It is less accurate to predict the discharge (Q) using the watershed (feature in the GIS) [32]. Anticipation of discharge prediction can use the Manning approach, using the elevation of irrigation (H) (see Table 1). Based on Table 1, the deviation of the prediction and measurement results is small (an average of 16.42%). Thus, mapping hydropower in pico scale can be done using GIS-based on DEMNAS Indonesia data for elevation (head) projections and Manning's approach for the discharge prediction.

Based on the assessment, two locations for the implementation of pico hydro have been identified, namely the undershot waterwheel for i_1 and the breastshot waterwheel for i_2. Both turbines are operated in environmental conditions (actual conditions). They have good performance, the η_{mech} for undershot of 24.3% (deviation to Denny's limit is 5.03%) and breastshot of 45.7% (deviation to Denny's limit is 4.53%). It shows that both turbines are possible as independent power plants for remote or rural areas, especially in Indonesia.

VII. Conclusion

This study aims to measure water energy on a pico scale as a regional resource of potential contribution as an independent power plant based on a topographical map and assess the suitable technology for these conditions. Based on the results, the advantages of pico hydro as the off-grid supply for remote or rural areas in Indonesia are promising. The utilization of GIS-based DEMNAS data for mapping the energy potential of water on a pico scale to accelerate the electrification process in remote areas is recommended, especially for Indonesia. The topographical maps made using GIS can be used as decision support because the irrigation elevation (head) is projected accurately and precisely. Consequently, a potential location is detected.

Furthermore, the discharge prediction results using Manning's approach are categorized as valid and verified; the difference with field measurements is 13.95%. Based on mapping results and discharge prediction, two locations are suitable for undershot waterwheel and breastshot waterwheel. Based on the results, both turbines have good performance; their peak mechanical efficiency is close to the limit (± 5%).

Acknowledgement

Thanks to Mr. Stevanus Nalendra Jati, M.Eng. from Study Program of Geological Engineering, Universitas Sriwijaya for help in reviewing describing data taken from GIS.

References

[1] Direktorat Jenderal Ketenagalistrikan, "Update Informasi (Sub Sektor Ketenagalistrikan)," Jakarta, 2019.

[2] International Energy Agency (IEA), "World Energy Outlook 2018: The Future is Electrifying," 2018.

[3] F. M. Sari, "PLN Kembangkan Pembangkit Listrik Tenaga Piko Hidro di Papua," Jakarta, 2019.

[4] S. K. Yudha, "PLN Gunakan Piko Hidro Terangi Desa di Papua," Jakarta, 2019.

[5] D. Adanta, Budiarso, Warjito, and A. I. Siswantara, "Assessment of turbulence modelling for numerical simulations into pico hydro turbine," *J. Adv. Res. Fluid Mech. Therm. Sci.*, vol. 46, no. 1, pp. 21–31, 2018.

[6] Budiarso, Warjito, M. N. Lubis, and D. Adanta, "Performance of a Low Cost Spoon-Based Turgo Turbine for Pico Hydro Installation," *Energy Procedia*, vol. 156, pp. 447–451, 2019.

[7] D. Febriansyah, Budiarso, Warjito, K. Watanabe, and D. Adanta, "Storage System Manufacturability , Portability and Modularity for a Pico Hydro Turbine," *J. Adv. Res. Fluid Mech. Therm. Sci.*, vol. 2, no. 2, pp. 209–214, 2018.

[8] Humas EBTKE, "Rasio Elektrifikasi 99,9% Tahun 2019," *Energi Baru Terbarukan dan Konservasi Energi (EBTKE)*, 2019. .

[9] M. Faizal, "Sepekan, Tim Ekspedisi Papua Terang Berhasil Survei 292 Desa," *Sindo*, Jakarta, 2018.

[10] Y. Kusdiantono, "4 Hari Menegangkan Demi Melistriki Pedalaman Sarmi," *Sindo2*, Jayapura, 18AD.

[11] A. A. Williams and R. Simpson, "Pico hydro–Reducing technical risks for rural electrification," *Renew. Energy*, vol. 34, no. 8, pp. 1986–1991, 2009.

[12] Badan Standardisasi Nasional, *Prosedur penentuan batas Daerah Aliran Sungai (DAS) untuk peta skala 1:250.000*, SNI 8200:2. Jakarta: Badan Standardisasi Nasional, 2015.

[13] Ardian Syah, *Manual Pembangunan PLTMH*. Jakarta: Japan International Cooperation Agency, 2017.

[14] D. P. Sari, Helmizar, I. Syofii, Darlius, and D. Adanta, "The Effect of the Ratio of Wheel Tangential Velocity and Upstream Water Velocity on the Performance of Undershot Waterwheels," *J. Adv. Res. Fluid Mech. Therm. Sci.*, vol. 65, no. 2, pp. 170–177, 2020.

[15] Budiarso, Helmizar, Warjito, A. Nuramal, W. Ramadhanu, and D. Adanta, "Performance of breastshot waterwheel in run of river conditions," in *AIP Conference Proceedings*, 2020, vol. 2227, no. 1, p. 20014, doi: https://doi.org/10.1063/5.0000940.

[16] M. R. Ramdhani, R. Irwansyah, Budiarso, Warjito, and D. Adanta, "Investigation of the 16 Blades Pico Scale Breastshot Waterwheel Performance in Actual River Condition," *J. Adv. Res. Fluid Mech. Therm. Sci.*, vol. 75, no. 1, p. 3847, 2020, doi: https://doi.org/10.37934/arfmts.75.1.3847.

[17] Dicky Davis, "Studi Eksperimental Unjuk Kerja Kincir Air Tipe Saluran Bawah (Undershot Water Wheel)," Universitas Bengkulu, 2018.

[18] S. J. Williamson, B. H. Stark, and J. D. Booker, "Low head pico hydro turbine selection using a multi-criteria analysis," *Renew. Energy*, vol. 61, pp. 43–50, 2014.

[19] G. Garegnani, S. Sacchelli, J. Balest, and P. Zambelli, "GIS-based approach for assessing the energy potential and the financial feasibility of run-off-river hydro-power in Alpine valleys," *Appl. Energy*, vol. 216, pp. 709–723, 2018, doi: https://doi.org/10.1016/j.apenergy.2018.02.043.

[20] A. Kuriqi, A. N. Pinheiro, A. Sordo-Ward, and L. Garrote, "Flow

regime aspects in determining environmental flows and maximising energy production at run-of-river hydropower plants," *Appl. Energy*, vol. 256, p. 113980, 2019, doi: https://doi.org/10.1016/j.apenergy.2019.113980.
[21] Y. Li, N. Lei, and Y. Xiong, "Research on watershed extraction method based on GIS," in *IOP Conference Series: Earth and Environmental Science*, 2019, vol. 300, no. 2, p. 22168, doi: 10.1088/1755-1315/300/2/022168.
[22] Badan Meteorologi, Klimatologi, dan Geofisika (BMKG), "Prakiraan Cuaca (Weather Forecast)," 2019. .
[23] Warjito, D. Adanta, S. B. S. Nasution, M. A. F. Kurnianto, and Budiarso, "The effect of blade height and inlet height in a straight-blade undershot waterwheel turbine by computational method," *CFD Lett.*, vol. 11, no. 12, pp. 66–73, 2019.
[24] Warjito, S. A. Arifianto, Budiarso, S. B. Nasution, and D. Adanta, "Effect of Blades Number on Undershot Waterwheel Performance with Variable Inlet Velocity," in *2018 4th International Conference on Science and Technology (ICST)*, 2018, pp. 1–6.
[25] E. Quaranta and R. Revelli, "Performance characteristics, power losses and mechanical power estimation for a breastshot water wheel," *Energy*, vol. 87, pp. 315–325, 2015, doi: http://dx.doi.org/10.1016/j.energy.2015.04.079.
[26] E. Quaranta and R. Revelli, "Optimization of breastshot water wheels performance using different inflow configurations," *Renew. Energy*, vol. 97, pp. 243–251, 2016, doi: 10.1016/j.renene.2016.05.078.
[27] E. Quaranta and R. Revelli, "CFD simulations to optimize the blade design of water wheels," *Drink. Water Eng. Sci.*, vol. 10, no. 1, p. 27, 2017.
[28] M. Denny, "The efficiency of overshot and undershot waterwheels," *Eur. J. Phys.*, vol. 25, no. 2, p. 193, 2003.
[29] N. F. Yah, M. S. Idris, and A. N. Oumer, "Numerical investigation on effect of immersed blade depth on the performance of undershot water turbines," in *MATEC Web of Conferences*, 2016, vol. 74, p. 35.
[30] E. Quaranta and G. Muller, "Optimization of undershot water wheels in very low and variable flow rate applications," *J. Hydraul. Res.*, vol. 58, pp. 1–5, 2019, doi: 10.1080/00221686.2019.1671508.
[31] Q. Emanuele and R. Roberto, "Hydraulic Behavior and Performance of Breastshot Water Wheels for Different Numbers of Blades," *J. Hydraul. Eng.*, vol. 143, no. 1, p. 4016072, Jan. 2017, doi: 10.1061/(ASCE)HY.1943-7900.0001229.
[32] S. N. Jati, S. R. O. Manik, D. P. Sari, and D. Adanta, "Feasibility of geoscience to determine the location of micro-hydro power potential for rural areas," *Int. Energy J.*, vol. 21, no. 1, pp. 41–56, 2021.

Dewi Puspita Sari was born in South Sumatera, Indonesia on July 27th 1987. Degree: B.Edu. (2010) in Mechanical Engineering Education from Universitas Sriwjaya, South Sumatera-Indonesia. M.Edu. (2014) in Technology Education, Universitas Sriwijaya, South Sumatera - Indonesia. She has been working as a lecturer for the Study Program of Mechanical Engineering Education, Faculty of Education and Teacher Training, Universitas Sriwijaya, South Sumatera, Indonesia. Dewi Puspita Sari, B.Edu., M.Edu. have publication had written in: Journal of Advanced Research in Fluid Mechanics and Thermal Science; International Energy Journal; International Journal of Fluid Machinery and Systems; and Journal of the Brazilian Society of Mechanical Sciences and Engineering.

Stevanus Nalendra Jati was born in North Kalimantan, Indonesia on August 30th 1989. Degree: B.Eng. (2011) in Geological Engineering from Universitas Pertahanan Veteran Yogyakarta, Yogyakarta-Indonesia. M.Eng. (2014) in in Geological Engineering from Universitas Pertahanan Veteran Yogyakarta, Yogyakarta-Indonesia.
He has been working as a lecturer for the Study Program of Geological Engineering, Faculty of Engineering, Universitas Sriwijaya, South Sumatera - Indonesia. Stevanus Nalendra Jati, B.Eng, M.Eng. have publication had written in: International Energy Journal; and Journal of Physics: Conference Series.

Imam Syofii was born in South Sumatera, Indonesia on November 19th 1983. Degree: B.Edu. (2005) in Mechanical Engineering Education from Universitas Negeri Semarang, Central Java - Indonesia. M.Eng. (2009) in Mechanical Engineering, Universitas Gajah Mada, Yogyakarta - Indonesia.
He has been working as a lecturer for the Study Program of Mechanical Engineering Education, Faculty of Education and Teacher Training, Universitas Sriwijaya, South Sumatera - Indonesia. Imam Syofii, B.Edu., M.Eng. have publication had written in: Journal of Advanced Research in Fluid Mechanics and Thermal Science; International Journal of Fluid Machinery and Systems; and Journal of the Brazilian Society of Mechanical Sciences and Engineering.

Dendy Adanta was born in South Sumatera, Indonesia, on June 5th, 1993. Degree: M.Eng. (2017) in Mechanical Engineering from Universitas Indonesia, Jakarta - Indonesia. Dr. (2020) in Mechanical Engineering, Universitas Indonesia, Jakarta - Indonesia.
He has been working as a lecturer for the Department of Mechanical Engineering, Faculty of Engineering, Universitas Sriwijaya, South Sumatera, Indonesia. Dr. Dendy Adanta, M.Eng. some publication had written in: International Journal of Technology; International Journal on Advanced Science, Engineering and Information Technology; CFD Letters; Journal of Advanced Research in Fluid Mechanics and Thermal Science; Energy Reports; Journal of Mechanical Engineering and Sciences; Engineering Letter; International Energy Journal; International Journal of Fluid Machinery and Systems; Journal of the Brazilian Society of Mechanical Sciences and Engineering; Malaysian Journal of Medicine and Health Sciences; and several seminar proceedings. Dr. Dendy Adanta, M.Eng. is memberships in professional societies in the International Association of Engineers (IAENG).